# Mossy fiber-evoked subthreshold responses induce timing-dependent plasticity at hippocampal CA3 recurrent synapses

Federico Brandalise and Urs Gerber[1]

Brain Research Institute, University of Zurich, CH-8057 Zurich, Switzerland

Dentate granule cells exhibit exceptionally low levels of activity and rarely elicit action potentials in targeted CA3 pyramidal cells. It is thus unclear how such weak input from the granule cells sustains adequate levels of synaptic plasticity in the targeted CA3 network. We report that subthreshold potentials evoked by mossy fibers are sufficient to induce synaptic plasticity between CA3 pyramidal cells, thereby complementing the sparse action potential discharge. Repetitive pairing of a CA3–CA3 recurrent synaptic response with a subsequent subthreshold mossy fiber response induced long-term potentiation at CA3 recurrent synapses in rat hippocampus in vitro. Reversing the timing of the inputs induced long-term depression. The underlying mechanism depends on a passively conducted giant excitatory postsynaptic potential evoked by a mossy fiber that enhances NMDA receptor-mediated current at active CA3 recurrent synapses by relieving magnesium block. The resulting NMDA spike generates a supralinear depolarization that contributes to synaptic plasticity in hippocampal neuronal ensembles implicated in memory.

analog signaling | hippocampal mossy fibers

The CA3 area of the hippocampus exhibits a distinctive, highly recurrent circuitry proposed to support autoassociative memory representation (1, 2). This prediction has been confirmed by experimental work demonstrating the pattern completion capabilities of CA3 networks (3), as well as their roles in the spatial tuning of CA1 pyramidal cells, in one-trial contextual learning (4) and in certain forms of memory consolidation (5). CA3 pyramidal cells receive, via the mossy fibers, information processed by granule cells important for both pattern separation (6, 7) and pattern completion functions (7). The faithful transmission of mossy fiber input appears to be ensured by giant synapses composed of presynaptic boutons with up to 45 release sites (8) that target massive spines, the thorny excrescences, on the apical dendrite of CA3 pyramidal cells. Thus, the mossy fiber synapse is often referred to as a detonator synapse (9). In fact, mossy fiber signaling is more compatible with a gatekeeper function than a high-throughput data relay. Although high-frequency bursts of action potentials in a hippocampal granule cell can discharge a targeted CA3 pyramidal cell, the majority of responses evoked by granule cells in CA3 pyramidal cells do not attain the firing threshold (10). Nevertheless, mossy fibers generate powerful signals evoking subthreshold responses that are much larger than typical synaptic events in the brain, with excitatory postsynaptic potentials (EPSPs) and excitatory postsynaptic currents (EPSCs) reaching amplitudes of 10 mV and 1 nA, respectively (11). Here we examined in rat slice cultures how EPSPs generated at mossy fiber synapses are processed in CA3 pyramidal cell dendrites, and evaluated whether subthreshold synaptic responses evoked by mossy fiber stimulation can act as instructive signals to induce plasticity at the pyramidal cell synapses forming the CA3 recurrent network.

## Results

We recorded evoked synaptic responses in single CA3 pyramidal cells voltage-clamped at $-70$ mV in which $GABA_A$ receptor-mediated responses were reduced with intracellular picrotoxin (1 mM). During pairing protocols, to induce synaptic plasticity, recordings were performed in current-clamp mode at resting potential ($-64.4 \pm 3.8$ mV; $n = 18$). One stimulating electrode was positioned in the CA3 stratum radiatum to stimulate recurrent afferents, and the other was placed in the dentate gyrus to activate mossy fibers (Fig. S1A), which form synapses on the trunk of the apical dendrite of CA3 pyramidal cells (12). The identity of the stimulated fiber tracts was ascertained using standard criteria (Fig. S1).

We studied synaptic plasticity at CA3 recurrent inputs. Plasticity was induced by pairing an evoked CA3 recurrent EPSP with a mossy fiber EPSP that followed with a delay of 10 ms, repeated 60 times at 0.1 Hz (Fig. 1A), comparable to standard spike timing-dependent plasticity (STDP) protocols (13). We chose this low frequency of stimulation because we were interested in studying plasticity solely at CA3 recurrent synapses, and thus avoided frequency facilitation and long-term potentiation (LTP) of mossy fiber-evoked responses ($-6.9 \pm 5.4\%$; $n = 18$; $P = 0.32$) (14). Furthermore, high-frequency mossy fiber stimulation evokes synaptic release of zinc (15), which can depress heterosynaptic potentiation at CA3 recurrent inputs (16).

CA3 recurrent synaptic EPSPs were enhanced during the pairing protocol (by $179 \pm 93\%$; $n = 18$; $P < 0.001$) (Fig. 1B and Fig. S2 A and B), whereas mossy fiber-evoked EPSPs remained unchanged. Action potentials were never observed at the stimulation intensities used (Figs. S2–S4). The potentiation of EPSCs at CA3 recurrent synapses persisted for more than 1 h, corresponding to LTP ($54.4 \pm 4.8\%$; $n = 18$ of 21; $P < 0.001$; 3 of 21

NEUROSCIENCE

**Fig. 1.** Pairing of subthreshold CA3 and mossy fiber responses induces plasticity at CA3 recurrent synapses. (*A*) Subthreshold pairing protocol for LTP induction in a CA3 pyramidal cell at resting potential, in which activation of a CA3 recurrent input is followed after 10 ms by activation of a mossy fiber input. Shown are the first (black) and last 10 averaged traces (red) of the 60 pairings. (*B*) Time course of responses during the pairing protocol in current-clamp mode. Mossy fiber-evoked EPSPs did not exhibit facilitation at the stimulation frequency of 0.1 Hz, whereas CA3 recurrent-evoked EPSPs were potentiated. (*C*) LTP induced at CA3 recurrent synapses in cells voltage-clamped at −70 mV, before and after the 10-min pairing protocol in current-clamp mode applied at time 0. Data points are values averaged over 3 min. Example traces show averaged EPSCs before (black) and after (red) repetitive pairing. (*D*) LTD was induced when the timing of the pairing was reversed such that the stimulation of the mossy fiber input preceded stimulation of the CA3 recurrent input by 35 ms. (*E*) Summary data for timing intervals of −35, 0, +10, and +40 ms. (*F*) Blocking sodium channels with QX-314 (500 μM) did not reduce heterosynaptic LTP.

cells did not exhibit plasticity) (Fig. 1*C*). A subsequent STDP protocol did not lead to any further significant enhancement of LTP (65.9 ± 8.7%; n = 3; P = 0.14).

If the timing of the inputs was reversed such that the delay between the evoked CA3 recurrent EPSP and the subthreshold mossy fiber EPSP was −35 ms, then long-term depression (LTD) was induced (reduction of 42.9 ± 8.5%; n = 5; P < 0.001) (Fig. 1*D*). When the pairing latency was zero or increased to +40 ms, no significant plasticity at the CA3–CA3 recurrent synapse was obtained (0 ms: 1.9 ± 9.4%; n = 4; P = 0.12; +40 ms: −5.5 ± 8.8%; n = 3; P = 0.18) (Fig. 1*E*). Blocking sodium channels with intracellularly applied QX-314 (17) did not significantly change the magnitude of LTP (65.7 ± 10.4%; n = 3; P = 0.18), confirming that action potentials are not required for this form of plasticity (Fig. 1*F*). Significant LTP was induced even when GABA$_A$ receptors were not blocked (Fig. S2 *E* and *F*). Furthermore, EPSP-dependent LTP exhibited input specificity (Fig. S3).

Synaptic plasticity at CA3 recurrent synapses is NMDA receptor-dependent (18–20), as is associative plasticity at CA3 recurrent synapses induced by mossy fiber-evoked spiking (21, 22). Thus, we tested whether EPSP-dependent LTP is also NMDA receptor-dependent. To evaluate the potential roles of NMDA receptors at

CA3 recurrent synapses and mossy fiber synapses separately, we used MK801 (40 μM), an irreversible use-dependent NMDA receptor antagonist. Our results indicate that activation of NMDA receptors at CA3 recurrent synapses, but not at mossy fiber synapses, is necessary for mossy fiber EPSP-dependent LTP (Fig. 2 *A*–*D*).

Previous investigations of heterosynaptic plasticity at CA3 recurrent synapses by mossy fiber stimulation used suprathreshold signals in the form of trains of action potentials (21, 22). In those studies, activation of extrasynaptic group I metabotropic glutamate (mGlu) receptors was involved in plasticity. In our experiments, heterosynaptic potentiation of CA3 recurrent synapses was achieved without mGlu receptor activation, because plasticity was not modified in the presence of a specific antagonist (MCPG 500 μM; 58.3 ± 13.6%; n = 3; P < 0.001), and the low-frequency, single-pulse pairing that we used resulted in negligible glutamate spillover to extrasynaptic receptors. Taken together with our observation that mossy fiber stimulation can be mimicked by a subthreshold voltage step applied to the CA3 pyramidal cell to induce LTP of comparable magnitude (Fig. 2 *E* and *F*), these findings are consistent with a passive electrical signal rather than a biochemical mechanism as the process underlying EPSP-dependent plasticity.

During the pairing protocol (i.e., before the development of LTP), arithmetic summation of the EPSPs was evoked by the CA3 recurrent input and the mossy fiber input in some trials, whereas in others, the summation was supralinear (34.3 ± 5.1%; n = 18) (Fig. 3*A*). These two distinct populations of response became readily apparent when traces were scaled to the amplitude of the evoked CA3 EPSP (Fig. 3*B* and Fig. S4), with supralinear response amplitude exceeding linear response amplitude by 96.9 ± 10.3% (n = 18; P < 0.001). Supralinear responses were almost completely blocked when NMDA receptors were antagonized pharmacologically (Fig. S5), suggesting that these events could be dendritic NMDA spikes, as originally described in cortical pyramidal cells (23–25). NMDA spikes were subsequently observed in hippocampal pyramidal cells as well (26, 27).

We then asked whether the mossy fiber EPSP is passively conducted distally along the dendrite to CA3 recurrent synapses to alleviate the magnesium block from NMDA receptors. If this were the case, then the likelihood of evoking an NMDA spike at a CA3 recurrent synapse should diminish as a function of the distance between the mossy fiber synapse and the CA3 recurrent synapse. As an indicator of the distance between the juxtasomatic mossy fiber input and the more distal CA3 recurrent input, we measured the rise time, under control conditions, of the somatically recorded CA3 EPSC (Fig. 3*C*, *inset*), which because of dendritic filtering declines with increasing distance from the site of the somatic recording electrode (28, 29). Plotting EPSC rise time against the magnitude of LTP induced at the CA3 recurrent synapse revealed a correlation (r = 0.66; P < 0.001) (Fig. 3*C*), suggesting that proximity of the CA3 input to the mossy fiber input is a critical factor for inducing EPSP-dependent LTP. A plot of EPSC rise time against the number (expressed in percent) of supralinear events evoked during the 60 pairings also revealed a positive correlation (r = 0.68; P < 0.001) (Fig. 3*D*). Furthermore, the number of supralinear events observed during the 60 pairings was correlated with the magnitude of LTP (r = 0.74; P < 0.001) (Fig. 3*E*). It is of particular interest that in the absence of supralinear events (<10% of 60 pairings; n = 4), LTP was never induced (Fig. 3*E* and Fig. S6).

We also observed a correlation between the EPSC rise time and the mean amplitude of supralinear events, calculated in relation to linear event amplitude, suggesting more effective activation of NMDA receptors at more proximal recurrent synapses compared with those at distal synapses (r = 0.69; P < 0.001) (Fig. 3*F*). Finally, after the induction of LTP with the pairing protocol, the probability of evoking a supralinear response was significantly increased (control: 38.7 ± 7.6%; after pairing: 67.3 ± 8.8%; n = 3; P < 0.05).

We further characterized the role of the supralinear response in inducing plasticity by recording from the trunk of the apical dendrite (Fig. 4*A*). After confirming that the response was dependent on NMDA receptor activation, we examined its timing
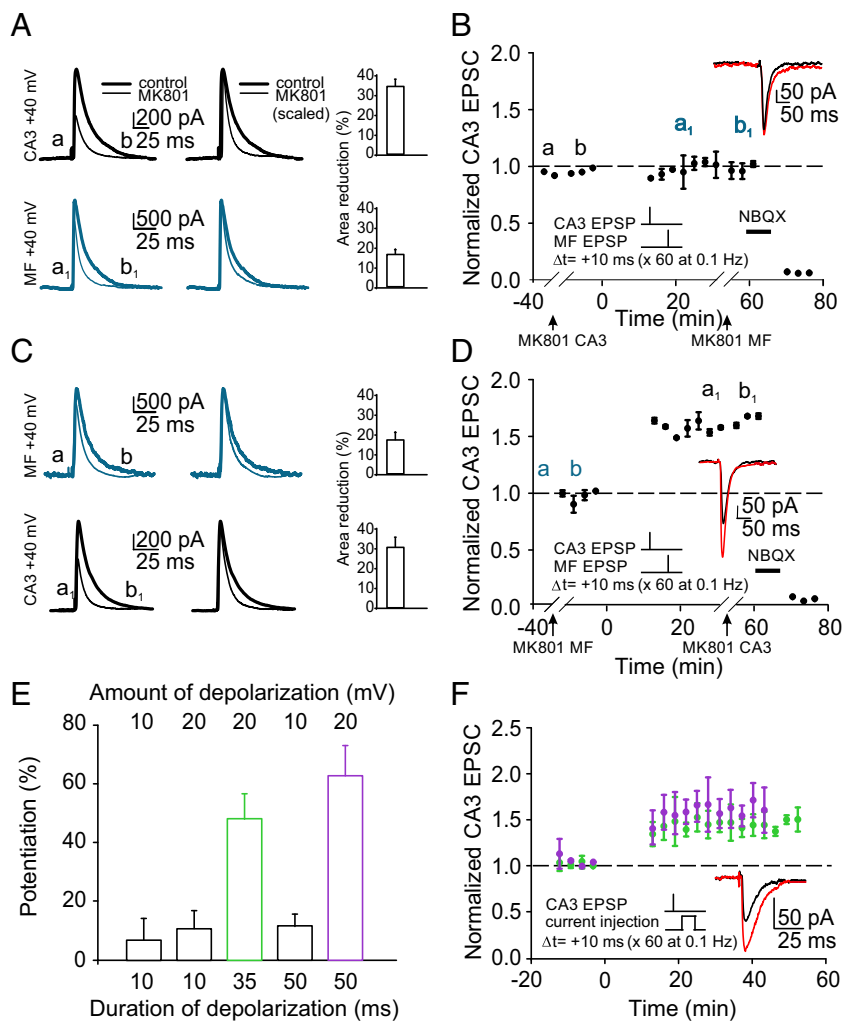
**Fig. 2.** The mossy fiber signal that induces EPSP-dependent LTP does not require activation of postsynaptic NMDA receptors and can be mimicked by passive current injection. (*A* and *B*) NMDA receptors were blocked selectively at the CA3 recurrent input (black traces, a, b) by application of the use-dependent antagonist MK801 in a CA3 pyramidal cell voltage-clamped at +40 mV (charge transfer reduced by $30.9 \pm 4.5\%$; $n = 3$). This prevented subsequent induction of LTP in current-clamp mode ($0.5 \pm 3.6\%$; $n = 3$; $P = 0.42$). A second application of MK801 at +40 mV reduced mossy fiber responses (blue traces, $a_1$, $b_1$) by $16 \pm 2.6\%$ ($n = 3$), similar to that seen in a previously unexposed cell ($17.9 \pm 4.1\%$; $n = 3$) (blue traces in C), demonstrating that the initial application of MK801 did not block mossy fiber NMDA receptors. (*C* and *D*) Use-dependent block of NMDA receptors only at mossy fibers (blue traces, a, b) had no significant effect on LTP ($50.4 \pm 3.6\%$; $n = 3$; $P < 0.001$) compared with control ($54.4 \pm 4.8\%$; $n = 11$; $P < 0.001$). Subsequent application of MK801 reduced the CA3 recurrent-evoked response by $29.1 \pm 3.6\%$ ($n = 3$), comparable to the reduction observed for an initial application ($P = 0.27$) (black traces in A). (*B* and *D*) NBQX (10 μM) blocked residual currents. (*E* and *F*) A subthreshold depolarization induced by current injection can substitute for mossy fiber stimulation, consistent with a mechanism involving electrotonic dendritic signaling. The magnitude of LTP is a function of the amplitude and duration of the stimulus.

properties (Fig. 4*B* and Fig. S7*C*). When the mossy fiber EPSP followed the CA3 recurrent EPSP by 10 ms, the amplitude of the supralinear responses recorded in the dendrite exceeded the amplitude of the mean linear responses by $115.8 \pm 11.1\%$ ($n = 9$; $P < 0.001$). A supralinear response was not observed when the timing of the inputs was set such that the mossy fiber EPSP preceded the CA3 recurrent EPSP by 35 ms, the timing used for LTD ($16.8 \pm 3.1\%$; $n = 5$; $P = 0.09$), or when the two inputs were activated synchronously ($-14.2 \pm 1.2\%$; $n = 4$; $P = 0.13$), conditions that did not induce potentiation.

If the hypothesis that EPSP-dependent LTP depends on an interaction occurring in the apical dendrite is correct, then the supralinear response would be expected to be more apparent in recordings from dendrites receiving clustered synaptic input compared with somatic recordings. Thus, we obtained simultaneous recordings from a first-order apical dendritic branch and from the soma (Fig. S8). In these experiments, it was possible to select a locus of stimulation that evoked a CA3 recurrent EPSP of greater amplitude in the dendritic recording than in the somatic recording (Fig. 4*D* and Fig. S8*C*). When we then paired the response with a mossy fiber-evoked EPSPs that followed at 10 ms, the percentage increase of the supralinear responses was always greater in the dendrite than in the soma (by $52 \pm 9.7\%$; $n = 6$; $P < 0.001$). In contrast, when a stimulation site was chosen that evoked a smaller EPSP in the recorded dendrite than in the soma, the magnitude of the supralinear responses was smaller in the dendritic recording compared with the somatic recording (by $42 \pm 9.7\%$, $n = 3$; $P < 0.005$; Fig. 4*E*).

The ratio in amplitude of the dendritic versus the somatic CA3 recurrent EPSP reflects the proximity of the dendritic recording electrode to the source of the supralinear response. Accordingly, we observed a correlation between dendritic/somatic CA3 recurrent EPSP amplitude and the magnitude of the dendritic supralinear response ($r = 0.81$; $P < 0.001$), compatible with findings identifying circumscribed dendritic segments as the functional units for clustered synaptic plasticity (30, 31).

We conclude that an NMDA receptor-mediated supralinear response, corresponding to a dendritic NMDA spike (23–27), is sufficient to induce LTP between CA3 pyramidal cells. In neocortical pyramidal cells, activation of multiple synapses (from 9 to 43) is necessary to evoke an NMDA spike (32–34). A similar mechanism is involved in the generation of the supralinear response in CA3 pyramidal cells. When a paired recording approach was used to excite a single CA3 recurrent axon, which activates fewer than 10 synapses per targeted pyramidal cell (35), repetitive pairing of the unitary CA3 recurrent EPSP with an evoked mossy fiber EPSP failed to induce LTP ($n = 4$) (Fig. S6).

Another characteristic of NMDA spikes is that they do not require activation of sodium or calcium channels (23–25). Similarly, we found that a supralinear NMDA receptor-mediated response was reliably induced in the absence of a calcium plateau, but we could evoke a calcium spike through a 20–30% increase in the stimulation intensity applied to the CA3 recurrent input and mossy fiber input to depolarize the CA3 neuron beyond $-30$ mV ($n = 4$) (Fig. S7 *A* and *B*). However, LTP was still induced in the presence of nifedipine (5 μM) to block

NEUROSCIENCE
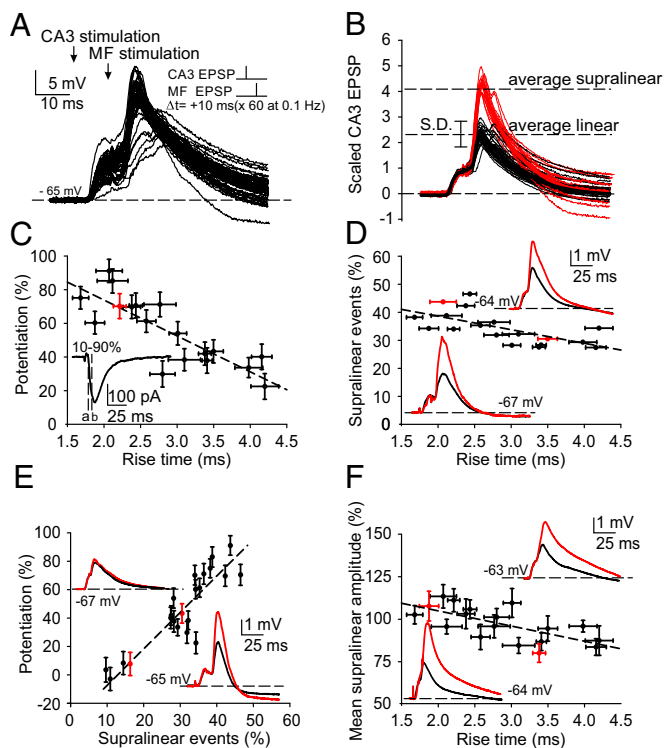
**Fig. 3.** Supralinear responses induced by pairing subthreshold CA3 recurrent and mossy fiber EPSPs. (*A*) Both linear and supralinear responses were induced during pairing of evoked EPSPs. (*B*) Illustration of the criterion used to distinguish between linear and supralinear summation of CA3 recurrent and mossy fiber evoked responses. Traces are scaled to the amplitude of the evoked CA3 recurrent EPSP, thereby revealing two discrete populations of responses. (*C*) A correlation is revealed when plotting the EPSC rise time, as a reflection of the distance between juxtasomatic mossy fiber input and more distal CA3 synaptic input, and the magnitude of LTP, suggesting that the proximity of CA3 input to mossy fiber input is critical for LTP induction. (*Inset*) Rise time measured from 10% of minimum (a) to 90% of maximum (b) of the EPSC evoked at −70 mV by stimulation of the CA3 recurrent input. The red data point corresponds to traces in the *Inset*. (*D*) EPSC rise time correlates with the probability of generating a supralinear response. (*Inset*) Averaged linear and supralinear responses. (*E*) The number of supralinear events evoked during the 60 pairings expressed in percent correlates with the magnitude of LTP, implicating the supralinear event as a causative factor. (*F*) EPSC rise time also correlates with the mean amplitude of the supralinear response.

high-threshold calcium channels (54.7 ± 17.6%; $n = 4$; $P < 0.001$) and nickel (50 μM) to block low-threshold calcium channels (52.4 ± 9.8%; $n = 4$; $P < 0.001$). Blocking sodium channels with QX-314 also did not prevent the supralinear NMDA receptor-mediated response, but did abolish the sodium spikelet and calcium plateau, even when stimulation strength was increased (Fig. S7 *B* and *C*).

## Discussion

The molecular processes underlying LTP/LTD expression induced by various established experimental protocols are well understood; however, the physiological conditions under which synaptic plasticity occurs remain unclear. Several previous studies have addressed this issue using STDP protocols, which correspond more closely to in vivo patterns of activity and follow timing-dependent contingencies of presynaptic and postsynaptic spikes as predicted by Hebb's rule for neural learning.

Central to STDP is the back-propagating action potential initiated in the postsynaptic cell that depolarizes the dendrites, thereby fulfilling a critical requirement for the activation of NMDA receptors; however, accumulating evidence suggests that for most forms of Hebbian plasticity, back-propagating action potentials are not essential and are in fact less effective than active dendritic responses in triggering synaptic plasticity (36). Furthermore, the STDP requirement for repetitive pairing of EPSPs and action potentials is problematic for plasticity involving mossy fiber synaptic input, because dentate granule cells in vivo exhibit very low levels of activity (6, 37, 38) and function as conditional detonators, evoking action potentials in a targeted CA3 pyramidal cell only infrequently (10). Here we propose that a subthreshold mechanism depending on mossy fiber-evoked EPSPs may compensate for the extreme sparseness of electrical activity in the granule cell population in vivo (6, 37–40).

Pairing of subthreshold synaptic responses has been shown to induce plasticity in a variety of neuronal circuits (13), a phenomenon variously referred to as EPSC-dependent LTP (LTP$_{EPSC}$) (41), subthreshold postsynaptic depolarization LTD (dLTD) (42), input-timing-dependent-plasticity (ITDP) (43), or subthreshold-depolarization dependent plasticity (SDDP) (44). The mossy fiber-dependent associative plasticity characterized in the present study represents an especially powerful form of subthreshold signal-induced plasticity. The exceptional effectiveness of the mossy input reflects on one hand its strategic localization at the base of the apical dendrite, where signals will passively propagate to depolarize more distal spines receiving CA3 recurrent input (12), and on the other hand the simultaneous release of large numbers of vesicles from a single terminal, essentially achieving cooperativity from a unitary fiber (8, 11). This production of a large AMPA receptor-mediated signal thus obviates the high-frequency temporal summation required to induce plasticity in most other circuits (45, 46). Furthermore, a large long-duration EPSP may be more efficient than a brief back-propagating action potential at counteracting the slow kinetics of magnesium unblock from NMDA channels (36, 47).

Our experiments show that the main determinant of heterosynaptic LTP induced by pairing evoked subthreshold potentials is a supralinear dendritic response. Candidate mechanisms for active dendritic responses are sodium spikes, calcium spikes, and NMDA spikes (48). Experiments with pharmacological blockers allow us to rule out sodium spikes and calcium spikes. Even though a calcium plateau could be evoked with stronger synaptic stimulation, such plateau potentials were never observed during our LTP protocol. In addition, dendritic calcium waves would not be triggered at the low frequency of mossy fiber stimulation that we used (49). Thus, by exclusion, the remaining candidate for the generation of a dendritic supralinear response is the NMDA spike.

Additional evidence for NMDA spikes is their sensitivity to specific antagonists and to hyperpolarization-induced block via magnesium, as well as the fact that they were evoked only when a critical number of NMDA receptor-containing synapses was activated within a given dendritic branch. Accordingly, NMDA spikes were observed with bulk stimulation, but not when a unitary input to a CA3 pyramidal cell was activated. Also facilitating the generation of NMDA spikes is the finding that NMDA receptors at CA3–CA3 synapses (50), as at CA1–CA3 synapses (51), conduct significant current at membrane potentials near resting potential.

Of note, numerous studies have shown that the induction of LTP by STDP depends ultimately on the generation of a supralinear dendritic response, rather than on the back-propagating spike per se (36). Thus, the dendritic mechanism for EPSP-dependent LTP and for STDP shares a common final step. Back-propagating spikes, as well as dendritic sodium and calcium spikes, are propagating signals, however, whereas NMDA spikes are restricted in their spatial extent by the requirement of glutamate binding to NMDA receptors. Thus, STDP may exert a more global effect within the dendritic tree than NMDA spike-dependent LTP.

The input timing requirements that allow subthreshold responses to induce synaptic plasticity may arise under a variety of physiological conditions. The CA3 pyramidal cell network

**Fig. 4.** The supralinear response evoked at CA3 recurrent synapses is mediated by an NMDA spike. (*A*) Image of a CA3 pyramidal cell during recording from the proximal apical dendrite. (Scale bar: 15 μm.) (*B*) A current-clamp recording from the apical dendrite (158 μm from the soma) in control conditions (before repetitive pairing) showing a supralinear summation of CA3 and mossy fiber-evoked responses. Traces are averages of 10 sweeps. The first two traces show averaged EPSPs evoked by a CA3 input and by a mossy fiber input alone. When mossy fiber stimulation follows CA3 stimulation with a delay of 10 ms, a supralinear response can be evoked. All traces with +10-ms pairings are scaled to the mean single-pulse CA3 EPSP. Supralinear summation is prevented by an NMDA receptor antagonist or by clamping the cell at −90 mV. (*C*) The timing of inputs is critical for induction of supralinear responses. A supralinear response is generated when a CA3 recurrent response is followed after 10 ms by a mossy fiber response, as in our LTP protocol (dendritic recording: 172 μm from the soma). Synchronous stimulation or a mossy fiber response preceding a CA3 recurrent response by 35 ms (as in the LTD protocol) does not produce a supralinear response. (*D*) Simultaneous recording from a first-order apical dendritic branch (upper traces) and from the soma (lower traces) showing averaged traces of a CA3 recurrent EPSP, a mossy fiber EPSP, a paired linear response, and a paired supralinear response. The greater amplitude of the signals in the dendritic recording indicates that for this cell, the synapses stimulated by the CA3 recurrent input are close to the recorded dendritic branch but far from the soma. In these cases, the supralinear response is greater (less attenuated) in the dendritic recording compared with the somatic recording. (*E*) In contrast, in cases where the stimulated CA3 recurrent input induces a smaller EPSP in the recorded dendrite than in the soma (dashed lines), the measured supralinearity is smaller in the dendritic recording than in the somatic recording. (*F*) Consequently, the magnitude of the supralinear responses recorded in the dendrite increases as a function of the ratio of the amplitude of the dendritic/somatic CA3 recurrent EPSP.
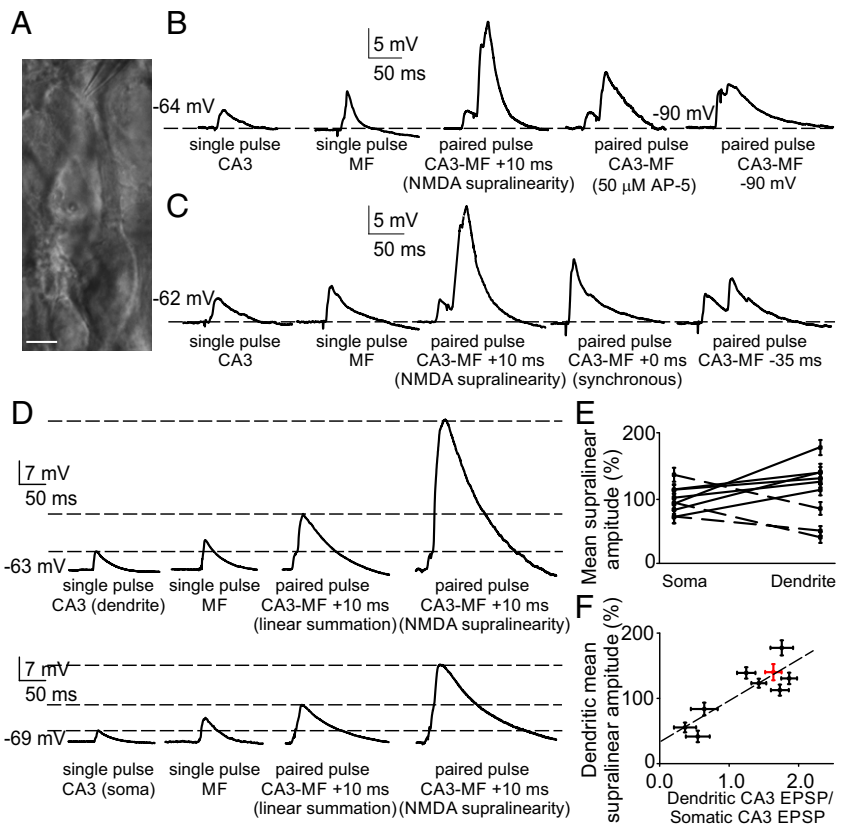
exhibits peaks of activity phase locked to theta oscillations (52); thus, when a given CA3 pyramidal cell receives theta-timed input from neighboring CA3 cells, appropriately timed subthreshold mossy fiber input would induce LTP. LTD would result if subthreshold mossy fiber input arrives before CA3 input, or asynchronously (53). Thus, the giant mossy fiber signal may operate as a gate directing CA3 recurrent synapses toward LTP or LTD, depending on the timing relationship of the inputs.

In conclusion, we have characterized a dendritic interaction that contributes to the induction of plasticity at CA3 recurrent synapses by generating NMDA spikes. The finding that EPSPs evoked by mossy fibers are sufficient to induce persistent changes in synaptic function provides further evidence of the importance of analog signaling in the nervous system, not only for the regulation of neurotransmitter release (54–56), but also for dendritic information processing and synaptic plasticity (43, 56–61).

## Materials and Methods

All experiments were performed in slice cultures prepared according to the Gähwiler method (62). Although there are slight modifications in the circuitry of slice cultures, these changes are apparent primarily in the CA1 area, whereas the connectivity of granule cells and the number of mossy fiber contacts in the CA3 area closely match the morphological characteristics observed in vivo (63). Slice cultures were prepared from 6-d-old Wistar rat pups killed by decapitation following a protocol approved by the Veterinary Department of the Canton of Zurich (approval ID 41/2011). In brief, 400-μm-thick hippocampal slices were fixed to glass coverslips using clotted chicken plasma, placed in sealed test tubes with serum-containing medium, and kept in a moving incubator at 36 °C for 21–28 d. Experiments were performed at 34 °C using the standard patch-clamp recording technique. All data are expressed as mean ± SEM.

**Electrophysiological Recordings.** Slice cultures were placed in a recording chamber mounted on an upright microscope (Zeiss Axioskop FS1) and superfused with an external solution (pH 7.4) containing 148.8 mM Na$^+$, 2.7 mM K$^+$, 149.2 mM Cl$^-$, 2.8 mM Ca$^{2+}$, 2.0 mM Mg$^{2+}$, 11.6 mM HCO$_3^-$, 0.4 mM H$_2$PO$_4^-$, 5.6 mM D-glucose, and 10 mg/L phenol red. All experiments were performed at 34 °C. Whole-cell recordings of CA3 pyramidal cells and dentate granule cells were obtained with patch pipettes (4–6 MΩ) filled with 135 mM K-gluconate, 5 mM KCl, 10 mM Hepes, 1 mM EGTA, 5 mM phosphocreatine, 2 mM MgATP, 0.4 mM NaGTP, and 0.07 mM CaCl$_2$ (pH 7.2). For the determination of current–voltage relationships, command potentials had a duration of 1 s to ensure steady-state responses. Data were recorded with an Axopatch 200B amplifier (Molecular Devices), digitized at 4 kHz for current-clamp and 5 kHz for voltage-clamp, and analyzed off-line with pCLAMP 10 (Molecular Devices) and Origin (Microcal Software). In some experiments, inhibitory postsynaptic potentials were reduced in the recorded CA3 pyramidal cells by adding picrotoxin (1 mM) to the patch solution. Series resistance (typically 5–15 MΩ) was monitored regularly, and cells were excluded if a change of >20% occurred during the recording.

**Drugs and Chemicals.** AP-5, MK801, NBQX, nifedipine, picrotoxin, QX-314, and S-MCPG were purchased from Abcam. ATP, phosphocreatine, EGTA, GTP, and nickel were purchased from Sigma/Fluka, and DCG-IV was purchased from Tocris Cookson.

**Data Analysis.** Data points for synaptic plasticity experiments are values averaged over 3 min. Thus, the first point plotted after the 10-min pairing protocol (60 times at 0.1 Hz) is at 13 min. Numerical data in the text are expressed as mean ± SEM. Statistical comparisons were performed using the Student $t$ test. Differences were considered significant at $P < 0.05$.

NEUROSCIENCE

1. McNaughton B, Morris RGM (1987) Hippocampal synaptic enhancement and information storage within a distributed memory system. *Trends Neurosci* 10(10): 408–415.
2. Rolls ET, Treves A (1990) The relative advantages of sparse versus distributed encoding for associative neuronal networks in the brain. *Network* 1:407–421.
3. Nakazawa K, et al. (2002) Requirement for hippocampal CA3 NMDA receptors in associative memory recall. *Science* 297(5579):211–218.
4. Nakashiba T, Young JZ, McHugh TJ, Buhl DL, Tonegawa S (2008) Transgenic inhibition of synaptic transmission reveals role of CA3 output in hippocampal learning. *Science* 319(5867):1260–1264.
5. Nakashiba T, Buhl DL, McHugh TJ, Tonegawa S (2009) Hippocampal CA3 output is crucial for ripple-associated reactivation and consolidation of memory. *Neuron* 62(6): 781–787.
6. Leutgeb JK, Leutgeb S, Moser MB, Moser EI (2007) Pattern separation in the dentate gyrus and CA3 of the hippocampus. *Science* 315(5814):961–966.
7. Nakashiba T, et al. (2012) Young dentate granule cells mediate pattern separation, whereas old granule cells facilitate pattern completion. *Cell* 149(1):188–201.
8. Rollenhagen A, et al. (2007) Structural determinants of transmission at large hippocampal mossy fiber synapses. *J Neurosci* 27(39):10434–10444.
9. Henze DA, Urban NN, Barrionuevo G (2000) The multifarious hippocampal mossy fiber pathway: A review. *Neuroscience* 98(3):407–427.
10. Henze DA, Wittner L, Buzsáki G (2002) Single granule cells reliably discharge targets in the hippocampal CA3 network in vivo. *Nat Neurosci* 5(8):790–795.
11. Bischofberger J, Engel D, Frotscher M, Jonas P (2006) Timing and efficacy of transmitter release at mossy fiber synapses in the hippocampal network. *Pflugers Arch* 453(3):361–372.
12. Amaral DG, Witter MP (1989) The three-dimensional organization of the hippocampal formation: A review of anatomical data. *Neuroscience* 31(3):571–591.
13. Feldman DE (2012) The spike-timing dependence of plasticity. *Neuron* 75(4):556–571.
14. Salin PA, Scanziani M, Malenka RC, Nicoll RA (1996) Distinct short-term plasticity at two excitatory synapses in the hippocampus. *Proc Natl Acad Sci USA* 93(23): 13304–13309.
15. Vogt K, Mellor J, Tong G, Nicoll R (2000) The actions of synaptically released zinc at hippocampal mossy fiber synapses. *Neuron* 26(1):187–196.
16. Ueno S, et al. (2002) Mossy fiber $Zn^{2+}$ spillover modulates heterosynaptic N-methyl-D-aspartate receptor activity in hippocampal CA3 circuits. *J Cell Biol* 158(2):215–220.
17. Connors BW, Prince DA (1982) Effects of local anesthetic QX-314 on the membrane properties of hippocampal pyramidal neurons. *J Pharmacol Exp Ther* 220(3):476–481.
18. Harris EW, Cotman CW (1986) Long-term potentiation of guinea pig mossy fiber responses is not blocked by N-methyl-D-aspartate antagonists. *Neurosci Lett* 70(1): 132–137.
19. Zalutsky RA, Nicoll RA (1990) Comparison of two forms of long-term potentiation in single hippocampal neurons. *Science* 248(4963):1619–1624.
20. Debanne D, Gähwiler BH, Thompson SM (1998) Long-term synaptic plasticity between pairs of individual CA3 pyramidal cells in rat hippocampal slice cultures. *J Physiol* 507(Pt 1):237–247.
21. Kobayashi K, Poo MM (2004) Spike train timing-dependent associative modification of hippocampal CA3 recurrent synapses by mossy fibers. *Neuron* 41(3):445–454.
22. Hunt DL, Puente N, Grandes P, Castillo PE (2013) Bidirectional NMDA receptor plasticity controls CA3 output and heterosynaptic metaplasticity. *Nat Neurosci* 16(8): 1049–1059.
23. Schiller J, Major G, Koester HJ, Schiller Y (2000) NMDA spikes in basal dendrites of cortical pyramidal neurons. *Nature* 404(6775):285–289.
24. Antic SD, Zhou WL, Moore AR, Short SM, Ikonomu KD (2010) The decade of the dendritic NMDA spike. *J Neurosci Res* 88(14):2991–3001.
25. Major G, Larkum ME, Schiller J (2013) Active properties of neocortical pyramidal neuron dendrites. *Annu Rev Neurosci* 36:1–24.
26. Wei DS, et al. (2001) Compartmentalized and binary behavior of terminal dendrites in hippocampal pyramidal neurons. *Science* 293(5538):2272–2275.
27. Makara JK, Magee JC (2013) Variable dendritic integration in hippocampal CA3 pyramidal neurons. *Neuron* 80(6):1438–1450.
28. Sayer RJ, Friedlander MJ, Redman SJ (1990) The time course and amplitude of EPSPs evoked at synapses between pairs of CA3/CA1 neurons in the hippocampal slice. *J Neurosci* 10(3):826–836.
29. Henze DA, Cameron WE, Barrionuevo G (1996) Dendritic morphology and its effects on the amplitude and rise-time of synaptic signals in hippocampal CA3 pyramidal cells. *J Comp Neurol* 369(3):331–344.
30. Govindarajan A, Israely I, Huang SY, Tonegawa S (2011) The dendritic branch is the preferred integrative unit for protein synthesis-dependent LTP. *Neuron* 69(1): 132–146.
31. Takahashi N, et al. (2012) Locally synchronized synaptic inputs. *Science* 335(6066): 353–356.
32. Larkum ME, Nevian T, Sandler M, Polsky A, Schiller J (2009) Synaptic integration in tuft dendrites of layer 5 pyramidal neurons: A new unifying principle. *Science* 325(5941):756–760.
33. Chalifoux JR, Carter AG (2011) Glutamate spillover promotes the generation of NMDA spikes. *J Neurosci* 31(45):16435–16446.
34. Oikonomou KD, Short SM, Rich MT, Antic SD (2012) Extrasynaptic glutamate receptor activation as cellular bases for dynamic range compression in pyramidal neurons. *Front Physiol* 3:334.
35. Mitra A, Mitra SS, Tsien RW (2012) Heterogeneous reallocation of presynaptic efficacy in recurrent excitatory circuits adapting to inactivity. *Nat Neurosci* 15(2):250–257.
36. Lisman J, Spruston N (2005) Postsynaptic depolarization requirements for LTP and LTD: A critique of spike timing-dependent plasticity. *Nat Neurosci* 8(7):839–841.
37. Jung MW, McNaughton BL (1993) Spatial selectivity of unit activity in the hippocampal granular layer. *Hippocampus* 3(2):165–182.
38. Wiebe SP, Stäubli UV (1999) Dynamic filtering of recognition memory codes in the hippocampus. *J Neurosci* 19(23):10562–10574.
39. Chawla MK, et al. (2005) Sparse, environmentally selective expression of Arc RNA in the upper blade of the rodent fascia dentata by brief spatial experience. *Hippocampus* 15(5):579–586.
40. Alme CB, et al. (2010) Hippocampal granule cells opt for early retirement. *Hippocampus* 20(10):1109–1123.
41. Krasteniakov NV, Martina M, Bergeron R (2004) Subthreshold contribution of N-methyl-D-aspartate receptors to long-term potentiation induced by low-frequency pairing in rat hippocampal CA1 pyramidal cells. *Neuroscience* 126(1):83–94.
42. Sjöström PJ, Turrigiano GG, Nelson SB (2004) Endocannabinoid-dependent neocortical layer-5 LTD in the absence of postsynaptic spiking. *J Neurophysiol* 92(6): 3338–3343.
43. Dudman JT, Tsay D, Siegelbaum SA (2007) A role for synaptic inputs at distal dendrites: Instructive signals for hippocampal long-term plasticity. *Neuron* 56(5):866–879.
44. Fino E, Deniau JM, Venance L (2009) Brief subthreshold events can act as Hebbian signals for long-term plasticity. *PLoS ONE* 4(8):e6557.
45. Buchanan KA, Mellor JR (2007) The development of synaptic plasticity induction rules and the requirement for postsynaptic spikes in rat hippocampal CA1 pyramidal neurones. *J Physiol* 585(Pt 2):429–445.
46. Sjöström PJ, Turrigiano GG, Nelson SB (2007) Multiple forms of long-term plasticity at unitary neocortical layer 5 synapses. *Neuropharmacology* 52(1):176–184.
47. Kampa BM, Clements J, Jonas P, Stuart GJ (2004) Kinetics of $Mg^{2+}$ unblock of NMDA receptors: Implications for spike-timing dependent synaptic plasticity. *J Physiol* 556(Pt 2):337–345.
48. Sjöström PJ, Rancz EA, Roth A, Häusser M (2008) Dendritic excitability and synaptic plasticity. *Physiol Rev* 88(2):769–840.
49. Kapur A, Yeckel M, Johnston D (2001) Hippocampal mossy fiber activity evokes $Ca^{2+}$ release in CA3 pyramidal neurons via a metabotropic glutamate receptor pathway. *Neuroscience* 107(1):59–69.
50. Debanne D, Guérineau NC, Gähwiler BH, Thompson SM (1995) Physiology and pharmacology of unitary synaptic connections between pairs of cells in areas CA3 and CA1 of rat hippocampal slice cultures. *J Neurophysiol* 73(3):1282–1294.
51. Kovalchuk Y, Eilers J, Lisman J, Konnerth A (2000) NMDA receptor-mediated subthreshold $Ca^{(2+)}$ signals in spines of hippocampal neurons. *J Neurosci* 20(5):1791–1799.
52. Mizuseki K, Royer S, Diba K, Buzsáki G (2012) Activity dynamics and behavioral correlates of CA3 and CA1 hippocampal pyramidal neurons. *Hippocampus* 22(8):1659–1680.
53. Debanne D, Gähwiler BH, Thompson SM (1994) Asynchronous pre- and postsynaptic activity induces associative long-term depression in area CA1 of the rat hippocampus in vitro. *Proc Natl Acad Sci USA* 91(3):1148–1152.
54. Alle H, Geiger JR (2008) Analog signalling in mammalian cortical axons. *Curr Opin Neurobiol* 18(3):314–320.
55. Christie JM, Chiu DN, Jahr CE (2011) $Ca^{(2+)}$-dependent enhancement of release by subthreshold somatic depolarization. *Nat Neurosci* 14(1):62–68.
56. Debanne D, Bialowas A, Rama S (2013) What are the mechanisms for analogue and digital signalling in the brain? *Nat Rev Neurosci* 14(1):63–69.
57. McNaughton BL, Douglas RM, Goddard GV (1978) Synaptic enhancement in fascia dentata: Cooperativity among coactive afferents. *Brain Res* 157(2):277–293.
58. Gustafsson B, Wigström H, Abraham WC, Huang YY (1987) Long-term potentiation in the hippocampus using depolarizing current pulses as the conditioning stimulus to single volley synaptic potentials. *J Neurosci* 7(3):774–780.
59. Artola A, Bröcher S, Singer W (1990) Different voltage-dependent thresholds for inducing long-term depression and long-term potentiation in slices of rat visual cortex. *Nature* 347(6288):69–72.
60. Golding NL, Staff NP, Spruston N (2002) Dendritic spikes as a mechanism for cooperative long-term potentiation. *Nature* 418(6895):326–331.
61. Hardie J, Spruston N (2009) Synaptic depolarization is more effective than back-propagating action potentials during induction of associative long-term potentiation in hippocampal pyramidal neurons. *J Neurosci* 29(10):3233–3241.
62. Gähwiler BH (1981) Organotypic monolayer cultures of nervous tissue. *J Neurosci Methods* 4(4):329–342.
63. Mori M, Abegg MH, Gähwiler BH, Gerber U (2004) A frequency-dependent switch from inhibition to excitation in a hippocampal unitary circuit. *Nature* 431(7007): 453–456.